Guo C, Song Y, Feng H, Zuo Z, Jia B, Zhang Z, Roskilly A.

Effect of fuel injection characteristics on the performance of a free-piston diesel engine linear generator: CFD simulation and experimental results.

***Energy Conversion and Management* 2018, 160, 302-312.**

Effect of fuel injection characteristics on the performance of a free-piston diesel engine linear generator: CFD simulation and experimental results

Chendong Guo[a], Yu Song[a], Huihua Feng[a,*], Zhengxing Zuo[a], Boru Jia[a,b], Ziwei Zhang[a], A.P. Roskilly[b]

[a] School of Mechanical Engineering, Beijing Institute of Technology, Beijing 100081, China
[b] Sir Joseph Swan Centre for Energy Research, Newcastle University, Newcastle Upon Tyne, NE1 7RU, UK

ARTICLE INFO

Keywords:
Free-piston diesel engine linear generator The injection timing
The injection rate-profile CDF simulation Experimental results

ABSTRACT

The free-piston diesel engine linear generator (FPDLG), as a novel energy conversion device, is investigated by many researcher groups. The injection characteristics are important for the FPDLG operation performance. Therefore, the effects of fuel injection characteristics on the FPDLG are researched by CDF simulation and experimental results in this paper. According to the results, it is found that the trends of the compression ratio and the peak in-cylinder pressure vs the injection timing are the identical with convex function curves. And the IMEP of the FPDLG also show the same trend. Although the heat-release rises in the rapid combustion period, the IMEP vs the injection timing various law present convex function curve on account of reduced heat-release in the normal combustion period. Four injection rate-profiles, i.e. rectangle, wedge, trapezium and triangle are si- mulated and compared. It is observed that the combustion process with the trapezium rate-profile curve is smoother. The peak in-cylinder pressure and the thermal efficiency can be kept high value while the center of heat-release curve near the TDC. Therefore the trapezium rate-profile is suggested is appropriate and can keep high efficiency of the FPDLG in order to get high engine efficiency.

1. Introduction

The free-piston diesel engine linear generator (FPDLG), as a novel energy conversion device, was researched, because of the background of low fuel consumption and stringent government emission legislation [1–6]. The FPDLG combines the free-piston diesel engines and the linear generator [7]. Its operation principle is that the high-temperature and high-pressure gas was produced after the heat-release process in the cylinder drives the mover (it combines the pistons and the generator moving magnet with connecting rod) to reciprocate, and the generator converts parts of the mover mechanical energy into electricity [2]. Without flywheel and crankshaft mechanism, so the FPDLG shows great differences with the conventional internal combustion engines (ICEs) in terms of the construction, operating performance, heat-release char- acteristics, etc. [8]. And the only significant moving component of the FPDLG is the mover, so that the friction loss will be reduced [9]. Meanwhile, due to the absence of the inertial structure and complex transmission mechanism which used to storing and delivering energy, the system efficiency is improved significantly [10,11]. In addition, higher partial-load efficiency and multi-fuel possibilities have been reported [12].

The free-piston engine concept was first introduced in the 1920s by Pescare, which was used as air compressors during that time [5,13]. In the following decades, researchers in German and French also applied it as gasifier and automotive, etc. [3,5,14]. The development of these engines was abandoned until the 1960s because the free-piston engine technology was viewed as not commercially feasible [14]. Recently, the free-piston engines were investigated by several world-wide research groups, such as West Virginia University, Sandia National Laboratory, German Aerospace Centre, Toyota central R&D Labs Inc., Newcastle University, and Beijing Institute of Technology.

Cristopher M. Atkinson et al. at West Virginia University developed a two-stroke spark ignition free-piston engine linear generator (FPLG) in the 1990s with the engine bore was 36.5 mm, maximum possible stroke was 50 mm [15–20]. The firstly studied the effect of the total heat input, the combustion duration, the reciprocating mass and the load on the operation of the linear generator via simulation models [17–19]. According to the simulation results, the peak in-cylinder gas pressure, the engine operation speed and the compression ratio, etc. showed significant cyclic variation. With the prototype system, they indicated that the output power of the larger bore engine can be in- creased to levels more suitable for hybrid vehicle propulsion [20].

* Corresponding author. Tel.: +86 10 6891 1062.
E-mail address: 7520170066@bit.edu.cn (H. Feng).

Dr. Peter Van Blarigan at Sandia National Laboratory presented the design of a dual piston FPLG with 30 kW electric power output. Meanwhile, the engine employed homogeneous charge compression ignition (HCCI) combustion mode operating on a variety of hydrogen- containing fuels. The experimental results demonstrated that the thermal efficiency was up to 56% with low emissions. The HCCI com- bustion process was found to be very rapid, approaching an almost constant-volume heat release process. The NO_x emissions level was predicted to be largely reduced compared with the conventional ICEs [21–22].

Researchers at the German Aerospace Centre (DLR) of Vehicle Concepts and Combustion Technology presented the FPLG as a compact electricity generation unit for application in hybrid electric vehicles based on a national development plan for electric mobility in 2009 [23–25]. To ensure stable operation of the system, the controller was developed and the control strategies, especially for the piston motion control, were evaluated. The designed FPLG system was consisted of two gas springs and a linear generator. It was applied as a range-ex- tender-unit which provided additional electric energy to electric ve- hicles in case of discharged batteries. In 2013, a complete autarkic FPLG system was taken into operation. Based on the experimental re- sults and the simulation results, they concluded that precise control of the ignition timing was essential for the stable operation of the FPLG [25].

Toyota central R&D Labs Inc. started to carry out research on the FPLG since 2013, and a two-stroke prototype was developed to study the operation characteristics and controlling strategies [26,27]. The researchers discussed the effect of the electric load and the ignition timing on the engine compression ratio based on the experimental re- sults and the simulation results. Both of the premixed charge com- pression ignition (PCCI) and spark ignition (SI) were applied on the prototype, and the output power, the engine indicated thermal effi- ciency and the compression ratio were obtained and compared. An output power of 10 kW was reported to be achieved, and the reached engine thermal efficiency was up to 42% in the PCCI combustion mode [27].

Roskilly and Boru Jia et al. at Newcastle University researched the FPLG by the mathematical model and the simulation results [10,11,28–32]. The dynamic cycle, the thermodynamic cycle and the operation performance of the engine were analyzed. The simulation results shown the parameters of the FPLG were highly coupled and nonlinear [10,11,28]. In order to further study the gas flow and the combustion process in-cylinder of the FPLG, they had carried out the three-dimensional model [29]. The simulation results demonstrated that the piston motion profile affect the gas flow in-cylinder, but the influence on the combustion process is not obvious. And the FPLG has advantages over the conventional ICEs in NOx emissions [30–32].

Zuo Zhengxing and Feng Huihua et al. at Beijing Institute of Technology have designed two types of the FPLG, namely spark ignition FPLG and compression ignition FPLG [1,2,4,5,7]. They researched the operation characteristics and the control strategies of the FPLG by si- mulation results and experimental results [1,4]. According to the earlier results, it shown that because of the low running frequency of the FPLG, the two-stroke engine has poor ventilation quality, the prototype could not run continuously during the generating process. However, the FPLG could achieve stable operation by improving the prototype, and the reasonable staring control strategy and switching control strategy were designed, the prototype could run smoothly in each working process [2,5,7]. And their main research was the stable operation and optimi- zation performance of the FPLG prototype.

Although several research institutes had done much work of the PFLG, there were the few prototypes which could run stably. Therefore, the lack of testing data leads to difficulties of researching the injection parameters on the FPDLG prototype. Meanwhile, the injection control methods of the conventional ICEs can't be applied on the FPDLG be-
cause of the unique operation characteristics. The injection timing is one of the key parameters which influence combustion characteristics [33]. Hence it affects the dynamic, the fuel economic and the emission properties of the diesel engine indirectly. Larger fuel injection advance angle lead to higher pressure rising rate which lead to crude operation of the engine, and low service-life of the engine. As for the key influence factor, this paper will focus on the influence of the injection char- acteristics on the engine performance of the FPDLG. This work has the following necessities:

(1) As the influence rule is explored, the injection parameters can be adjusted to improve the FPDLG efficiency and fuel economy when the designing prototype.
(2) The injection controlling strategies can be formulated based on the simulation results and experimental results.

Therefore, the FPDLG prototype and test bench is designed and established, and the experimental results can be obtained by setting various the injection timing. Also, the CFD model is developed and modified according to the experimental results to maintain good si- mulation accuracy. With the model, the injection timing and the in- jection rate-profile which can't be set in experiment will be considered and discussed as the variable. According to the results in this paper, the fuel injection characteristics study provides a useful guidance for the design and control of the combustion process in order to achieve the system performance optimization of the FPDLG.

2. FPDLG system description

2.1. *Prototype configuration*

In order to investigate the injection characteristics of the FPDLG, a two-stroke FPDLG prototype is developed showed in Fig. 1. The pro- totype is consisted of two free-piston diesel engines, a commercial linear motor/generator, fuel supply system, scavenging system, control system, etc. [7]. The mover that the pistons are connected to the moving magnet of the commercial motor/generator rigidly, which is the only significant moving component of the prototype. The whole operation process of the FPDLG includes the engine starting process and the generating process. The mover is driven by the linear motor/gen- erator during the starting process, and will be switched to a generator during the stable generating process under the action conversion system [2]. The main design parameters and the linear motor/generator parameters are described in Table 1.

As a novel energy conversion device, the requirements for the fuel supply system of the designed direct-injection FPDLG prototype are special. Firstly, the injection pressure should be high enough to ensure good fuel atomization effect. At the same time, the fuel injection parameters such as the injection timing, the fuel injection rate-profile and the injection amount should be able controlled and easily con- trolled during the engine operating process. A high-pressure common rail system is chosen as the fuel supply system. It includes a fuel tank, a filter, a high-pressure oil pump, several oil pipes and two injectors shown in Fig. 1. By designing the injection system and matching in- jection signal process system, several injection parameters such as the fuel injection amount for each cycle and the injection timing can be changed via the PC [7].

The testing bench is designed and adjusting to monitor or acquisi- tion data as shown in Fig. 1. To obtain the real-time in-cylinder gas pressure, the Kistler sensor is selected and applied in the test bench. The parameter of the mover (piston) displacement can be measured by the built-in encoder of the linear motor/generator. The measuring range of the encoder is from 0 mm to 260 mm, and the sensitivity is 0.02 mm. When collecting testing data, the National Instruments equipment and the LabView software are applied in the test bench [1,2,7]. The type of
main test devices and sensors are listed in Table 2.

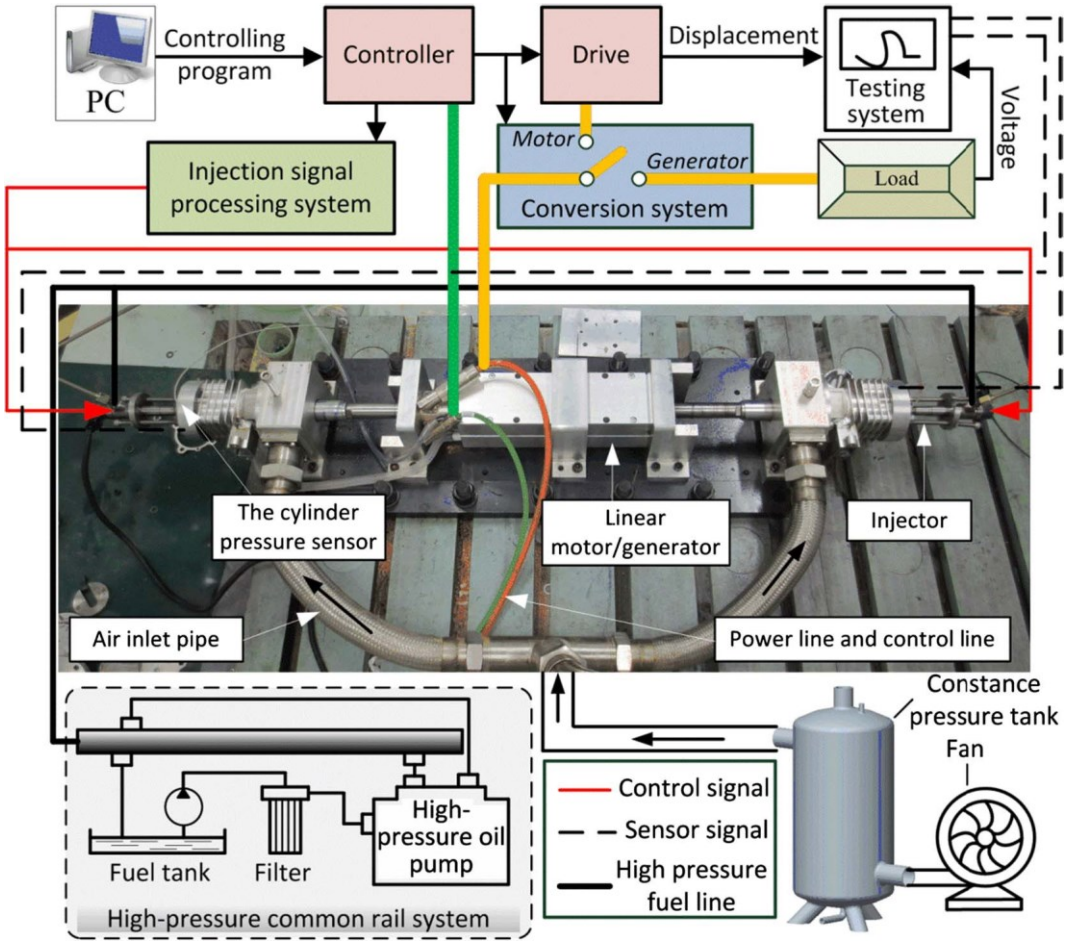

Fig. 1. The FPDLG prototype system and test bench.

Table 1
Main parameters of the FPDLG.

Parts	Parameters [Unit]	Value
Engines	Cylinder bore [mm]	60.00
	Maximum effective stroke [mm]	61.50
	Maximum total stroke [mm]	98.00
	Mass of the mover [kg]	6.00
	Fuel injection timing [mm]	6–10
	Pressure in common rail tube [Mpa]	100
	Scavenge temperature [K]	296
	Scavenge pressure [bar]	1.24
Linear motor/generator	Back EMF constant of generator [V/(m·s^{-1})]	76.00
	Internal resistance of coils [Ω]	5.40
	Peak force [N]	2162
	Maximum velocity [m/s]	5.9
	Peak current [A]	34
	Coil current [A]	20
	Force constant [N/A]	89.9

Table.2
Sensors type used in the experiment.

Test device	Type
Cylinder pressure sensor	Kistler 6052C
Gas pressure sensor	Kistler 4007BA5
Piston position sensor	Motor built-in encoder
Charge amplifier	Kistler 5018A1000
DAQ card	National Instruments

2.2. System operation principle test results

The operation process of the FPDLG prototype is illustrated in Fig. 2. The linear motor/generator runs as a motor that provides electro- magnetic force during the FPDLG starting process. The engine is control to start in one stroke as the working power and frequency of the linear motor we choose is large enough. Detailed introduction on the starting process can be found in our previous publications [34,35]. When the starting process is completed, the conversion system, as shown in Fig. 1, is triggered by the signal from the controller, and the working mode of the linear motor/generator is converted to a generator. The linear motor/generator runs as a generator afterwards. At the same time, the high-pressure common rail system and the scavenging system are en- abled. Parameters such as in-cylinder gas pressure and the piston dis- placement are also taken as feedback signals. If the engine compression ratio doesn't meet the requirement for combustion and misfire occurs, several systems will be disabled and the linear motor/generator will be operated as a motor to restart the prototype.

During the operation process, experimental results of the piston displacement and in-cylinder gas pressure in real-time coordinate are presented in Fig. 3. It can be seen that, during the engine starting process, the in-cylinder pressure of both sides engine can reach to 6 Mpa in the first cycle. Then the conversion system is triggered. At the same time, the scavenging and injection system are enabled, and combustion taken place in each cylinder alternative. Experimental re- sults of the in-cylinder pressure and the piston displacement are shown in Fig. 3. It is obviously that the in-cylinder pressure is relatively stable, and the peak value can reach up to 8 Mpa during the generating pro- cess. The engine operation frequency is approximately 26.3 Hz, which

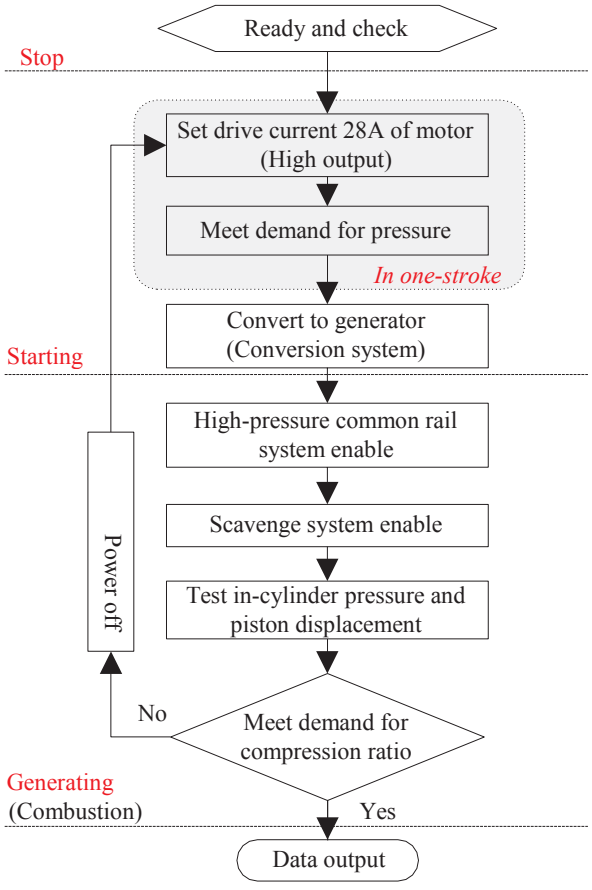

Fig. 2. Operation process of the experimental operation.

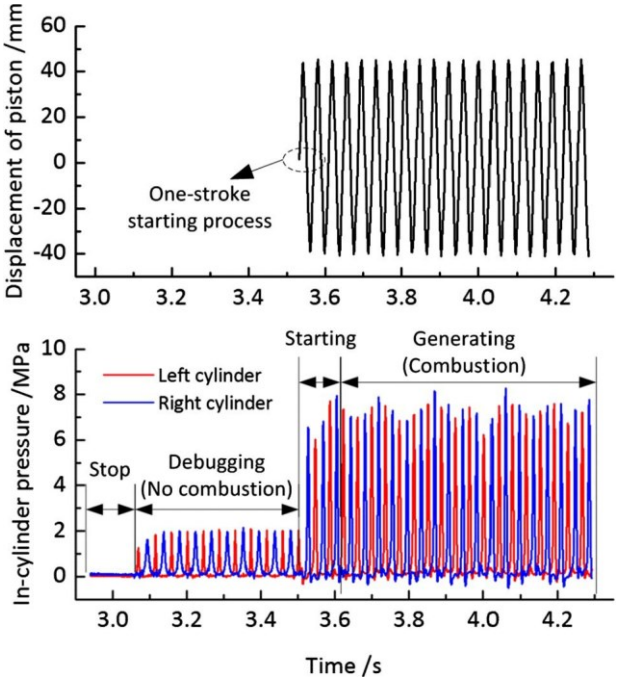

Fig. 3. Experimental results of the piston displacement and in-cylinder pressure.

is increased by 14.3% compared with that during the starting process.

2.3. *Analysis on different injection timing*

Due to the elimination of the crankshaft mechanism, the injection

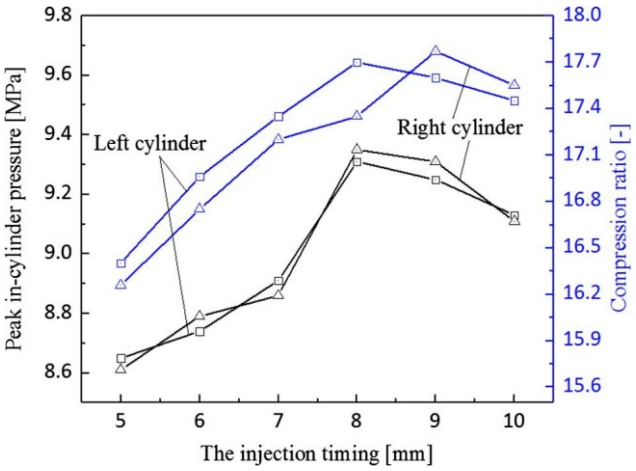

Fig. 4. Experimental results of peak in-cylinder pressure and the compression ratio with different injection timing.

timing of the FPDLG cannot be defined in the crank angle as the conventional ICEs. According to the FPLDLG operation characteristics, the injecting timing is defined as the distance from the piston top to the cylinder head for the FPDLG. During the test process of the FPDLG, the injection timing is set as 5–10 mm from the cylinder head. It can be seen that the peak in-cylinder pressure of both cylinders increases when the injection timing enlarge from 5 mm to 8 mm, as shown in Fig. 4. It is obvious that the time length for atomization, evaporation and mixture of oil spray becomes longer. However, the pressure and the temperature in cylinder are higher when the injection timing larger. With this effect, the quantity of combustible mixture gas and premix fuel is lower, so that the peak in-cylinder pressure reduces.

However, when the injection timing varies from 8 mm to 10 mm, the peak in-cylinder pressure decreased along with the injection timing increased, as shown in Fig. 4. And the trend of the engine compression ratio vs the injection timing is the same as the peak in-cylinder pressure shown in Fig. 4. This is because that the in-cylinder pressure and temperature are low during these fuel injection timing. So the in-cy- linder pressure and temperature don't meet the ignition condition, re- sulting in the fuel and the air pre-mixing duration is longer during the pre-mixing process. During the ignition delay period, the fuel touch the cylinder wall and the turbulent energy in-cylinder become worse with the injection timing increase. Thus, the peak in-cylinder pressure and the compression ratio both decrease when the injection timing increase. The Indicated Mean Effective Pressure (IMPE) vs the injection timing is calculated shown in Fig. 5. As the value of the injection timing increase, the IMEP of both cylinder increases firstly then drops. This conclusion also verifies the above explanation which related with ne- gative work. When the injection timing is set to 8 mm and then 9 mm, the mixture effect of gas and diesel is better to promote premix com- bustion quality. It is indicated that the output power of the FPDLG show the same trend of the IMEP vs the injection timing, so that there is a best injection timing in different operating frequency.

3. Simulation model and validation

3.1. *Simulation method*

In order to research the heat release characteristics in various of the injection timing and the injection rate-profile, the zero-dimension and CFD model are used during the simulating process. The zero-dimension can be used to simulate macroscopic piston movement and other working process characteristics of the FPDLG. The CFD model not only is used to compute characteristics of the heat release in cylinder, but also is applied on simulate the in-cylinder flow and distribution of the

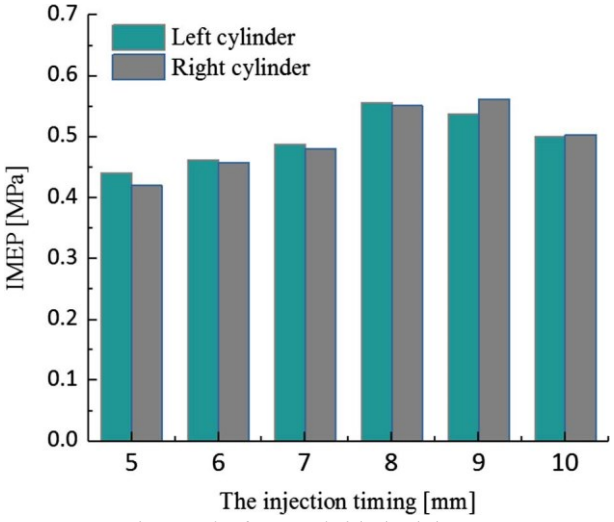

Fig. 5. Results of IMEP vs the injection timing.

oil spray characteristics. By adjusting parameters such the premix and the diffusive combustion quality factors, the models can be checked and the accuracy of it can be improved. With these adjusted models, the heat release characteristics of the different combustion phases in dif- ferent the injection timing and the injection rate-profile can be ob- tained.

3.1.1. Zero-dimensional model

When establishing combustion heat release model, the Wiebe function as a semi-empirical equation is applied on calculating and processing the test data. The single Wiebe function is always appro- priate for intermediate or low speed diesel engine. However, in order to improve the precision of the researching FPDLG prototype, the double- Wiebe function is applied on the simulation models [33]. The com- bustion percentage is replaced as $X = X_1 + X_2$ for simplifying. The function can be revised as (1).

$$\begin{cases} X = X_1 + X_2 \\ X_1 = \left\{1-\exp\left[-6.908 \times \left(\frac{t}{t_p}\right)^{m_p+1}\right]\right\}(1-Q_d) \\ X_2 = \left\{1-\exp\left[-6.908 \times \left(\frac{t}{t_z}\right)^{m_d+1}\right]\right\}Q_d \end{cases} \tag{1}$$

where t is time, X_1 is the premix combustion percentage, X_2 is the diffusive combustion percentage, m is the combustion quality factor, Q is the fuel mass fraction. Subscript p means the premix combustion process, and d means the diffusive combustion process. It considers the combustion process as a superposition effect of the premix and the diffusive combustion. So the ratio of the combustion heat release can be described as (2)

$$\frac{dX}{dt} = (1-Q_d)\left\{\frac{6.908(m_p+1)}{t_p} \times \left(\frac{t}{t_p}\right)^{m_p} \times \exp\left[-6.908 \times \left(\frac{t}{t_p}\right)^{m_p+1}\right]\right\} + Q_d\left\{\frac{6.908(m_d+1)}{t_z} \times \left(\frac{t}{t_z}\right)^{m_d} \times \exp\left[-6.908 \times \left(\frac{t}{t_z}\right)^{m_d+1}\right]\right\} \tag{2}$$

3.1.2. CFD model

According to the FPDLG prototype model, the geometry of the en- gine is established in the form of a computational mesh. Since grid quality of the CFD models influences on the computation speed and results precision significantly, meshing size and grid quality are two primary factors which affect simulation results. The smaller meshing size makes higher precision, but more grids cause more computation time. According to the combustion chamber configuration in our pre- vious paper, meshing size is set 4 times of nozzle diameter [7]. The volume mesh of the combustion chamber structure can be meshed, as shown in Fig. 6. At the beginning of the compression process, the total mesh number of cylinder is 70,686. During the piston moving process, the gradient mesh of the combustion chamber changes with the varia- tion of the piston displacement. In order to simulating the in-cylinder gas pressure and the combustion characteristics, the dynamic mesh is established according to the piston motion profile which is calculated with zero-dimension model. In this way, the final dynamic mesh is obtained in Fig. 6.

Without crankshaft and flywheel, the performance parameters of the FPDLG are not relative to crank-angle of crankshaft. When gen- erating dynamic mesh model, the piston motion profile in coordinate of crank-angle is needed to convert into description of the piston move- ment. However, neither the test data nor simulation results are in co- ordinate of time or displacement [33]. Therefore, the piston motion profile should be transformed to new expression in coordinate of the angle by using Eq. (3).

$$\begin{cases} x = r\left[(1-\cos\theta) + \frac{\lambda}{4}(1-\cos 2\theta)\right] \\ \omega = \frac{v}{r\left(\sin\theta + \frac{\lambda}{2}\sin 2\theta\right)} \end{cases} \tag{3}$$

where x is the piston displacement, v is the piston velocity, θ is the equivalent crank-angle, ω is the equivalent speed, r is the equivalent

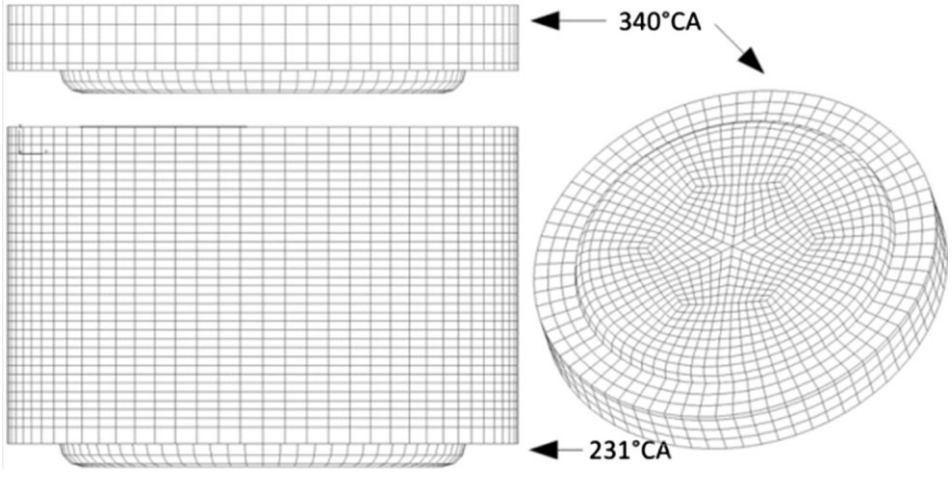

Fig. 6. The CFD model of combustion process.

Table 3
Key parameters for CFD model.

Parameters [Unit]	CFD model
Initial crank-angle of compression process [°CA]	61.0
Ending time of expand process [°CA]	290.6
Initial crank-angle of injection [°CA]	164.9
Distance between injection position and head [mm]	7
Injection angle [°CA]	140
Fuel mass [mg]	6.75
Fuel temperature [K]	296
Initial pressure in cylinder [bar]	1.24
Initial temperature in cylinder [K]	314

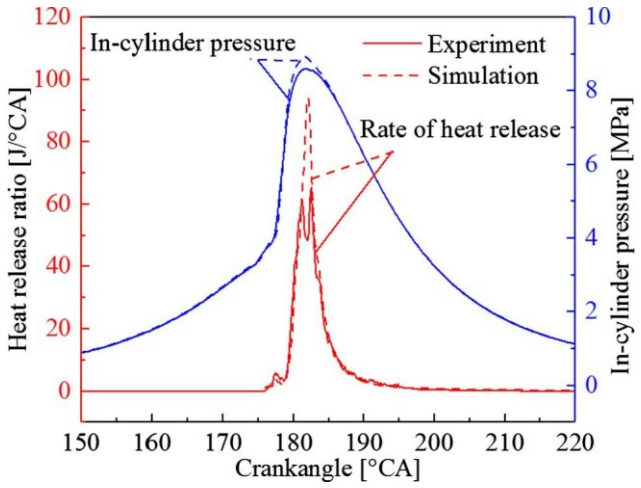

Fig. 7. In-cylinder pressure and heat release rate compared with simulation results and experimental results.

crank length and λ is the equivalent ratio of crank-rod. x and v can be obtained with zero-dimension model, and the crank-angle θ will be calculated with above equation set. By using this method, the injection
starting timing can be transformed to 164.9 °CA when the initial piston from the injection position to the cylinder head is 5 mm. Several parameters that required in the CFD model such as the initial crank- angle of the compression process are calculated and listed in Table 3.

3.2. Validation results

With the numerical model, the simulation results of the heat-release rate and the in-cylinder pressure are compared with the experimental results, as shown in Fig. 7. The objective function is established based on the least square theory, and the parameters are optimized. As the simulation results, the fitted curve of combustion heat release rate dX/dt is compared with the experimental data. It is observed that the si- mulation model can predict the general trends of the heat-release rate, while the peak value varies. The empirical value of the conventional ICEs is evaluated from 40 °CA to 60 °CA, but this value is larger than actual combustion duration of the FPDLG. Therefore, the duration in simulation model is adjusted as 5.5–8.3 ms in frequency of 22 Hz.

The mean square error of contrast error is 96.31, with a relative error of 6.79%. The combustion quality factor m_p of premix is set to 3.451, which is higher than that of the conventional ICEs based on the two reasons:

(1) The intake pressure is 1.24 bar, which is maintained by constant pressure tank in Fig. 1. With the designed scavenging system, the FPDLG is similar with a turbocharged and intercooled engine. As a result, the combustion process is delayed.
(2) Although the lower speed of the conventional ICEs results in higher m_p, experimental results show that the speed of 1440 r/min also leads to higher premix combustion proportion.

Table.4
Parameters setting of the five injection timing.

Injection timing [mm]	Compression ratio	Equivalent speed [r/min]	Injection timing [°CA]
5	16.40	1344	171.1
6	16.75	1530	168.9
7	17.15	1686	164.4
8	17.65	1800	159.5
9	18.10	1891	152.7

The combustion percentage Q_d of diffusive is 0.14 which is con- sistent with conclusion that 80% of fuel consumes in rapid during the combustion period. The combustion quality factor m_d of diffusive is set to 10.24. This is because the quantity of heat release is fewer and the appearance of the peak value delays.

4. Simulation results and discussion

4.1. Different injection timing

To analyze the heat release characteristics of the FPDLG during the combustion process, the CFD model is firstly applied to simulate in different the injection timing. Five injection timing, as shown in Table 4, are researched in the simulating process. And as the initial pressure is 1.14 bar, the initial temperature is 314 K, the injection angle is 140 °CA, the cycle fuel injection mass is 7 mg, and the injection duration is 1 ms. The injection timing of 10 mm is not used in the si- mulation as the corresponding output work is not optimized from the experimental results.

The data in Fig. 8 shows the influence of the fuel injection timing to in-cylinder gas pressure and in-cylinder gas temperature respectively. The results indicate that both of the peak in-cylinder pressure and temperature rise along with the growing the injection timing. And the crank-angle between the peak points of in-cylinder pressure and tem- perature enlarges as well. According to the experimental results, when the injection timing is set to 9 mm and 5 mm respectively, the peak in- cylinder pressure occurs in crank-angle of 178.7 °CA and 180.9 °CA, and the peak temperature occurs in crank-angle of 181.3 °CA and 191.4 °CA. By taking the combustion process division method of the conventional ICEs as a reference, it is considered that the normal combustion period of the FPDLG elongates with the decreasing of the fuel injection ad- vance timing, and more fuel is consumed on this stage. When the in- jection timing is set to 9 mm, earlier the injection timing leads to higher

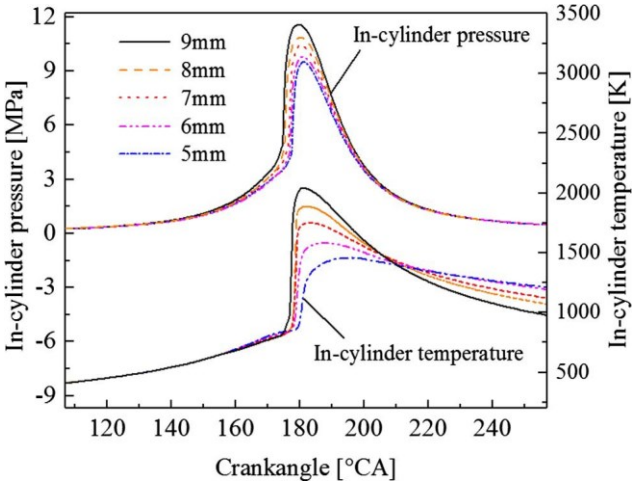

Fig. 8. In-cylinder pressure and temperature with different injection timing.

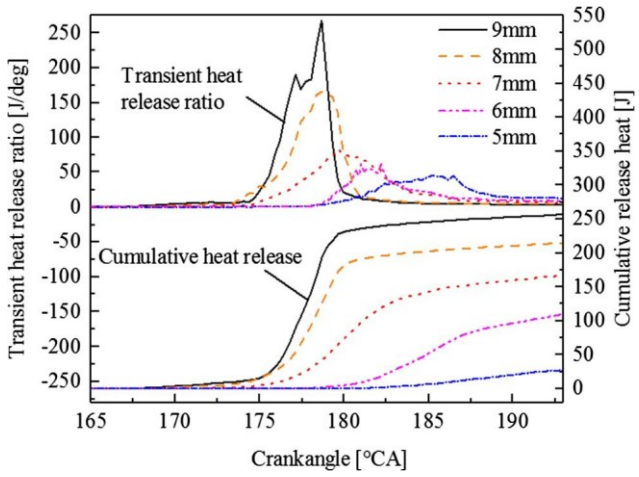

Fig. 9. Transient and cumulative heat release rate with different injection timing.

piston velocity in the initial stage of the compression stroke. So the pressure rising rate is the largest. In the later stage of the expansion stroke, the piston velocity is higher. Therefore the in-cylinder tem- perature declines and faster.

The results of the transient heat-release ratio and the cumulative heat-release are obtained and shown in Fig. 9. With earlier the injection timing, the curves of transient and cumulative heat-release rate become steeper. The results trend is the same as the experimental results when the injection timing increases from 5 mm to 8 mm. All of the phenom- enon indicate that the proportion of the premix combustion period raises along with increasing the injection timing. Amount of heat re- leased after the ignition delay period. With the simulation results, the ignition timing is delayed as the injection timing reduces. The ignition characteristics are influenced by two factors such as the injection timing and the gas-diesel mixture quality. Therefore the heat release curves and the ignition delay features are obtained as follows.

In addition, as for the in-cylinder pressure and temperature char- acteristics, the ignition delay period is another important influential factor during the combustion process. That is because the amount of the combustible mixture before the ignition timing has a close relation with the length of the ignition delay period. Since most of the fuel is burnt during the rapid combustion period for the free-piston engine, it will be crucial to control the length of the ignition delay period in order to control the combustion process of the FPDLG and reduce the mechan- ical load to make it run smoothly. To be specific, increasing the injec- tion timing brings about that the in-cylinder temperature and pressure

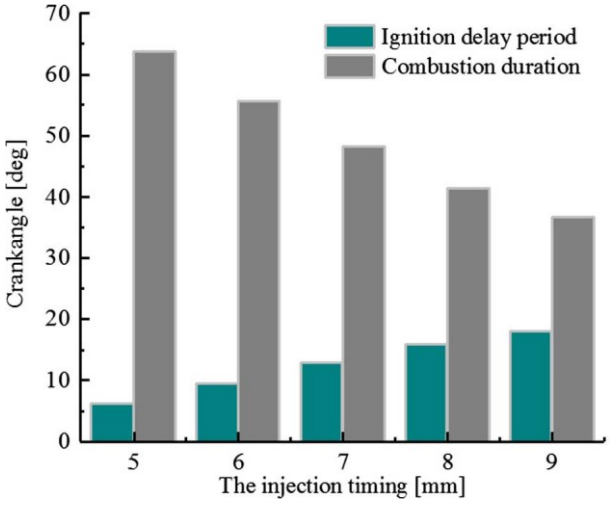

Fig. 10. Ignition delay period and combustion duration with different injection timing.

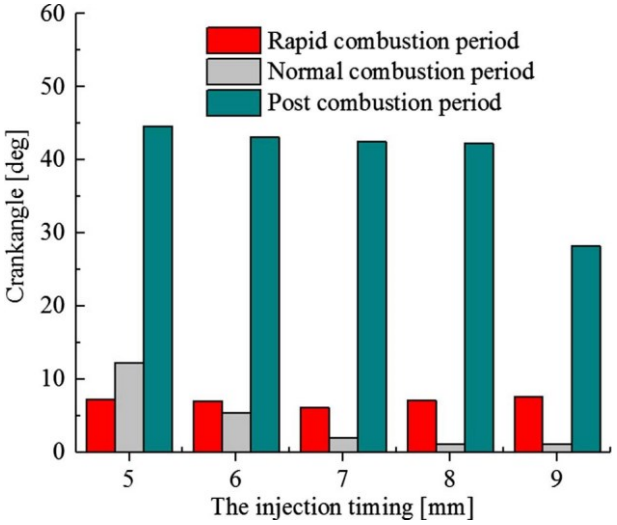

Fig. 11. The duration angle of each combustion period in different injection starting timing.

are simultaneously lower at the timing of injecting, and the ignition delay period will be longer. Although the in-cylinder gas temperature and pressure are higher when the injection timing decreases, the igni- tion delay period is shorter. Thus the piston may begin to move down at the time of ignition. It can be seen in Fig. 10 that the ignition delay period gets longer with the earlier injection timing.

The combustion duration is the crank angle from the time when combustion takes place to the time when the released heat reaches 95% of its maximum value. As shown in Fig. 10, the combustion duration measured in crank angel is gradually reduced with earlier the injection timing. Because advance of the fuel injection position caused the in- crease of the piston speed, mean the equivalent set rotate speed in- creases, the combustion duration measured in time changes more ob- viously with the changing of the fuel injection timing. With the fuel injection timing change from 5 mm to 9 mm, the ignition delay period decrease from 8.06 ms to 3.53 ms, declined by 1.28 times.

Fig. 11 illustrates the duration of each combustion stage in different injection starting timing. The rapid combustion period has no sig- nificant changes as more in advance of injection timing, only changing between 6.1 °CA and 7.6 °CA within a certain range of 6.58%. The normal combustion period shows a reductive trend in Fig. 11 as the injection timing increases from 5 mm to 9 mm. It changes from 12.2 °CA to 1.1 °CA with a percentage of 90.0%. These indicate that with the increasing of the fuel injection timing, the continuous time decease sharply from the peak pressure to peak temperature in the cylinder. The crank-angle of the post combustion period reduces from 44.6 °CA to 28.3 °CA. Although the descend percentage reaches to 36.5%, this period occurs at the fuel injection timing of 8–9 mm. In the point of 9 mm, the transient heat release close to zero after the TDC in Fig. 9. But it's clear that other curves last a long time when the transient heat release greater than zero after the TDC.

The released heat shown in Fig. 12 can reflect thermodynamic process of the FPDLG in cylinder. This value in rapid combustion period continues to increase from 112.29 J to 240.8 J with an increased per- centage of 114.4% as more advance of injection timing. This is caused by more cumulative mixed combustible gas which is prepared in igni- tion delay period. It can be calculated that releasing heat percentage in rapid combustion period of the total increases from 35.1% to 75.25%. This variation also confirms that more advance of injection timing lead to higher percentage of premixed combustion volume and lower dif- fusion combustion volume. For normal combustion period, the release heat reduces from 89.9 J to 4.98 J with a percentage of 94.5%. This related to shorter duration of the period which is described in Fig. 12.

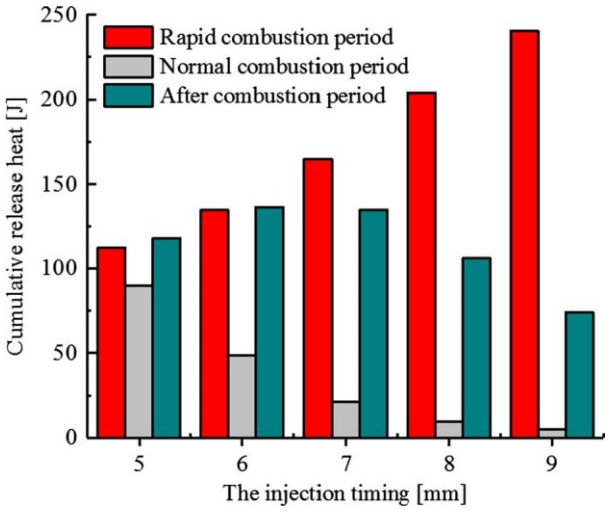

Fig. 12. Cumulative heat release in different combustion period.

Post combustion is an obvious characteristic of the FPDLG. Although the releasing heat in post combustion period takes larger proportion, the value in this period has no significant change. Specifically, the percentage of it rises from 23.2% to 42.6% as the injection timing in- crease from 5 mm to 8 mm. However, this percentage reduces to 36.8% as the injection timing increases continually to 9 mm. The reason is that the increase rate of combustion chamber volume is greater in expansion stroke comparing with conventional ICEs. The rapid decline of in-cy- linder pressure and temperature results in bad combustion condition.

4.2. *Different injection rate-profile*

The different injection rate-profile affects the combustion heat-re- lease process significantly through causing different barycenter of the heat release curve, the peak in-cylinder pressure, the peak temperature and the thermal efficiency. In order to increase the FPDLG operation efficiency by optimize the engine combustion performance, the dif- ferent injection rate-profile will be applied and upload to the CFD model to analyze the working process characteristics in cylinder. So that the four injector rate curves such as rectangle, wedge, trapezium and triangle will be set as shown in Fig. 13. In addition, the injection angle is set from 165 °CA to 180 °CA, the fuel injection mass of each cycle is 14 mg, the equivalent speed is 1686 r/min, the initial pressure is
1.14 bar and the initial temperature is 314 K.

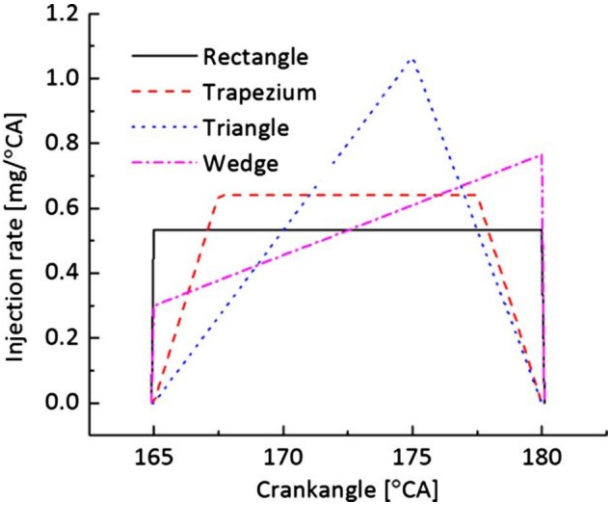

Fig. 13. Four fuel injection rate-profile profiles.

The influence of the injection rate-profile curves on the ignition delay period will be research by simulation. The length of ignition delay period related to formative time of mixed gas directly. The data in Fig. 14 shows the spray sauter diameter and heat release rete nepho- gram.

(1) The oil droplet diameter in frontal surface of spray is larger in fuel injection law of the triangle when the crank angle is 170 °CA. This is because the injection rate is speed up in mid-term of the injection process. The oil droplet sprayed into cylinder in early and late of the injection process mix together and generator larger diameter of droplets.
(2) As the piston moves from 170 °CA to 175 °CA, parts of droplets always attach the wall and rebound. However, it can be seen that most of droplets moves along generatrix of piston bowl and break into smaller diameter droplets. Then the combustible mixture gas accumulates in the bottom and middle of combustion chamber.
(3) With a crank-angle of 180 °CA, combustion occurs in the piston larynx in injection curves of the rectangle and the trapezium. When the curve is set as triangle, amount of oil spray burns in larynx and outside extend of the piston. For injection curve of the wedge, most of oil is injected into cylinder around TDC. Oil spray and air not mix fully before piston moving downward. Therefore combustion rate is low and more fuel burns in the middle of combustion chamber.

After setting the injection starting timing, the parameters relate to the ignition delay are obtained and listed in Table 5.

The various fuel injection mass during the combustion delay period is generated by different injection rate-profile. The in-cylinder pressure and temperature are shown in Fig. 15. The least injection mass can be achieved with wedge rate-profile. On the initial stage of rectangle rate- profile, the injection rate is higher, so that the in-cylinder pressure reaches to the peak point of 9.58 Mpa firstly. Nevertheless, more fuel that injected into cylinder leads to a higher peak pressure of 10.57 Mpa. As for the wedge rate-profile, the injection rate in the later period is greater, so that proportion of the post combustion is smaller and the peak in-cylinder pressure is lower. And the temperature curves in Fig. 15 also verify the same conclusion. The transient heat release rate results in Fig. 16 illustrates that the peak value of the triangle rate- profile is largest, and it is 3.2 time than the value of wedge rate-profile. The fuel equivalence ratio nephogram from 175 °CA to 190 °CA is shown in Fig. 17. With a crank-angle of 175 °CA, the fuel equivalence ratio in frontal surface of spray is higher when the injection rate-profile is triangle or wedge. Then it declines rapidly, and the fuel is consumed nearly in 180 °CA of the triangle curve. In 185 °CA, unburnt fuel con-centrates in the centre of the combustion chamber. But there is higher fuel equivalence ratio in local area as the nephogram of the rectangle and the wedge shown in Fig. 17. In 190 °CA of the rectangle and the wedge curves, the post combustion phenomenon is obvious, and the combustion efficiency is low.

From the discussions above, several rules and the key points in different injection rate-profile curve can be indicated.

(1) Rectangle: The spray in rectangle rate-profile start burning is ear-liest, and the peak in-cylinder pressure is highest.
(2) Triangle: Transient heat release ratio too high, so that the engine runs crudely.
(3) Wedge: The post combustion phenomenon is serious, and the bar-ycenter of heat release curve keep away from TDC. Therefore, the engine works smoothly, and the thermal power conversion effi-ciency is low.
(4) Trapezium: The barycenter of heat release curve near the TDC while the peak in-cylinder pressure is kept high. So the combustion effi-ciency is high.

Comparing with the conventional ICEs, the turbulence intensity in

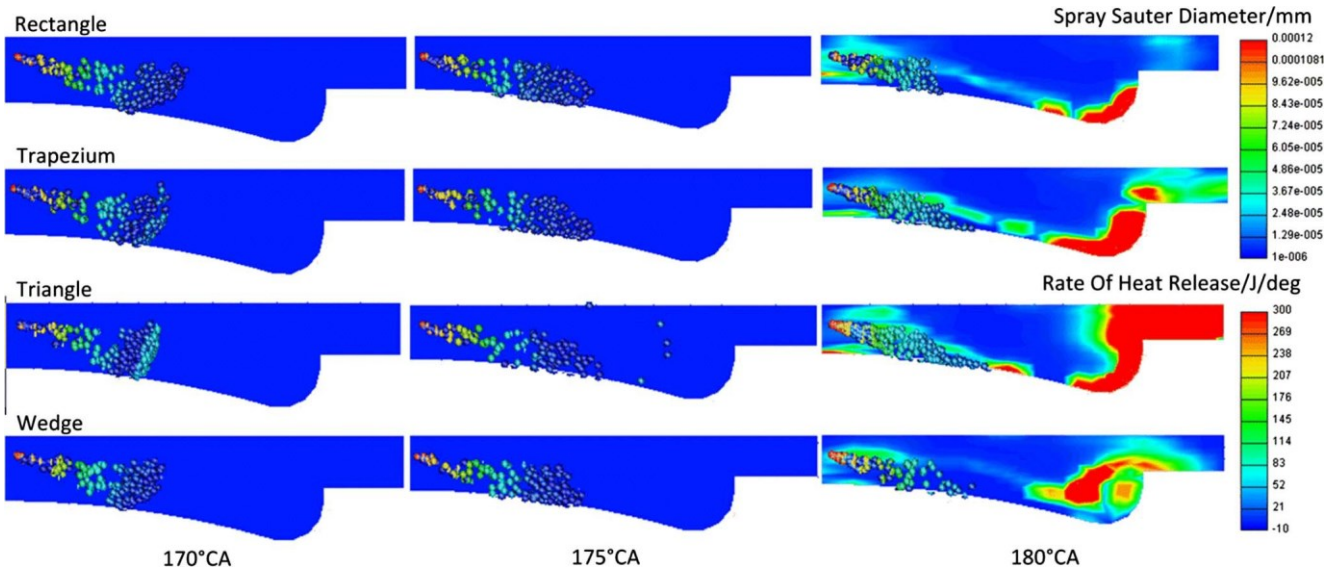

Fig. 14. Spray sauter diameter and rate of heat release nephogram.

Table 5
Key points and parameters relate to ignition delay.

Injection parameters	Rectangle	Trapezium	Triangle	Wedge
Starting point of injection [°CA]	165	165	165	165
Ignition point [°CA]	174.4	175	175.5	174.9
Ignition delay period [°CA]	9.4	10	10.5	9.9
Fuel-injection mass in delay period [mg]	5.01	5.6	5.83	4.56

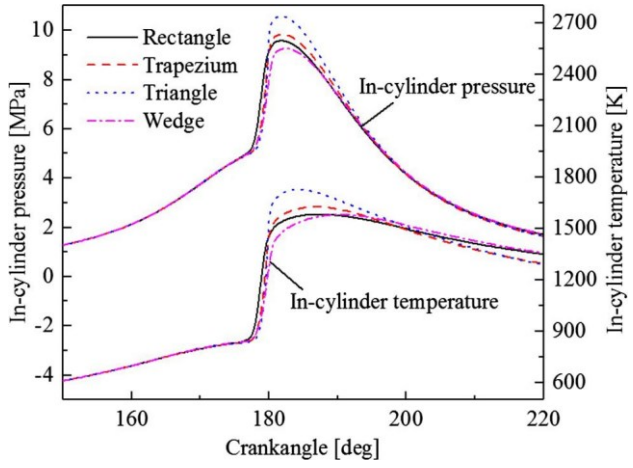

Fig. 15. In-cylinder temperature and pressure with the different injection rate-profile.

cylinder before the piston reaching to TDC is larger, and the mixing speed of gas and oil is faster. So that the effect of the different injection rate-profile on combustion heat release is more significant. Higher in- jection rate in earlier stage of the injection process leads to higher heat release. At the same time, the piston of the FPDLG moves faster after TDC, and the injection rate in wedge rate-profile is lower in later stage of the injection process. Finally, this condition will lead to more serious phenomenon of post combustion and low combustion efficiency.

5. Conclusion

The influence of injection characteristics on heat release of the FPDLG is investigated by simulation and experimental results base on the prototype test bench. One stroke starting strategy is applied to start

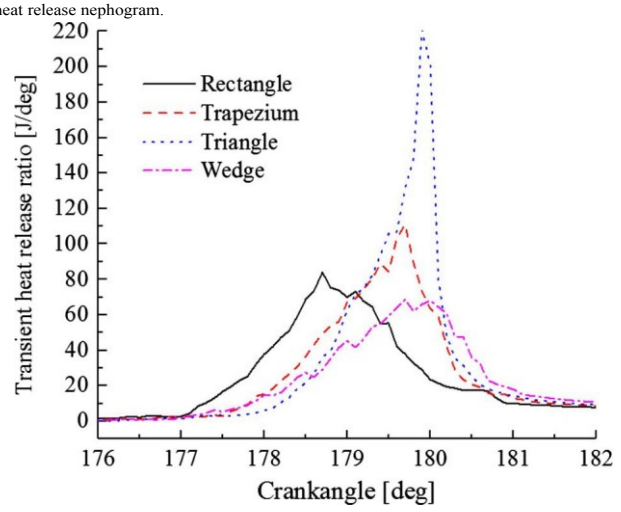

Fig. 16. The transient heat release rate profiles with different injection rate-profile.

the FPDLG, and the linear motor/generator ran as a motor to drive the piston to reach the required compression ratio for combustion. Both of the various the injection timing and the rate-profile are researched with the CFD model and experimental results.

Based on the experimental results from the prototype, the trends of the compression ratio and the peak in-cylinder pressure vs the injection timing are the convex function curves. And the IMEP of the FPDLG also has same trend. There is the maximum value is the fuel injection timing of 8 mm or 9 mm. That is because the better oil and gas mixing effect and the higher proportion of the premixed combustion period.

According to the united simulation model, the formation reasons can be analyzed. As the increasing of the injection timing, the duration of normal combustion period becomes shorter. In initial stage of the compression stroke and later stage of the expansion stroke, the pressure rising ratio improves faster. When the injection timing reaches to 8 mm, much less fuel is consumed in this period, and the combustion release heat reduces by 94.5%. Although the combustion release heat raises in rapid combustion period, the IMEPE vs the injection timing various law present convex function curve under the comprehensive effect.

The heat release characteristics in the four injection rate-profile such as the rectangle, the wedge, the trapezium and the triangle are researched. With the rate-profile of triangle, the peak transient heat release rate is too high. The post combustion phenomenon with the

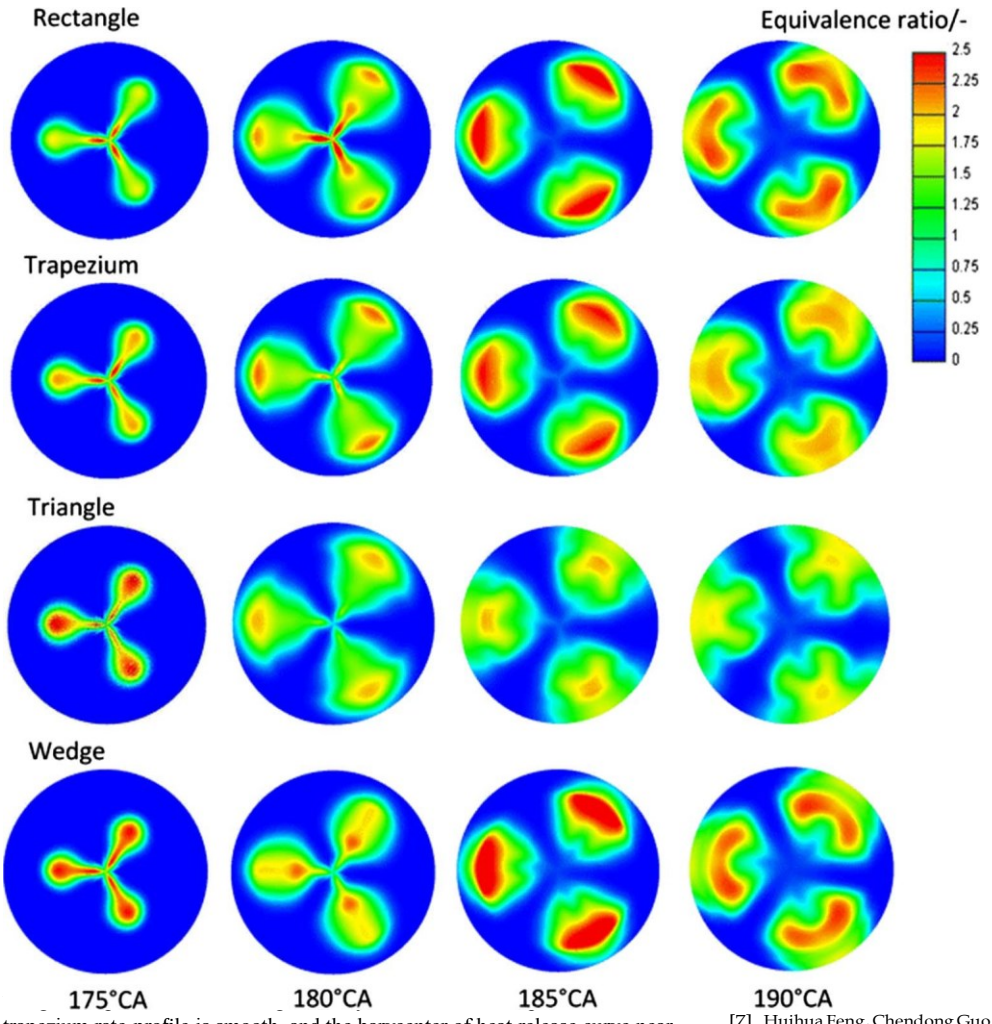

Fig. 17. Fuel equivalent ratio nephogram with different injection rate-profile.

trapezium rate-profile is smooth, and the barycenter of heat release curve near the TDC while the peak in-cylinder pressure is kept high. Therefore this rate-profile can keep high efficiency of the FPDLG.

Acknowledgements

This project is supported by the National Nature Science Foundation of China (51675043) and Programme of Introducing Talents of Discipline to Universities of China (B12022). We would like to thank the sponsors.

References

[1] Chendong Guo, Huihua Feng, Jia Boru, et al. Research on the operation characteristics of a free-piston linear generator: numerical model and experimental results. Energy Convers Manage 2016;122:153–64. http://dx.doi.org/10.1016/j.enconman.2016.05.068.

[2] Huihua Feng, Chendong Guo, Jia Boru, et al. Research on the intermediate process of a free-piston linear generator from cold start-up to stable operation: numerical model and experimental results. Energy Convers Manage 2016;122:153–64. http://dx.doi.org/10.1016/j.enconman.2016.05.068.

[3] BaHungOcktaeckLim Nguyen. A review of free-piston engines. Appl Energy 2016;178:78–97. http://dx.doi.org/10.1016/j.apenergy.2016.06.038.

[4] Boru Jia, Zuo Zhengxing, et al. Development and validation of a free-piston engine generator numerical model. Energy Convers Manage 2015;91:333–41. http://dx.doi.org/10.1016/j.enconman.2014.11.054.

[5] Jia Boru, Smallbone Andrew, et al. Design and simulation of a two- or four-stroke free-piston engine generator for range extender applications. Energy Convers Manage 2016;111:289–98. http://dx.doi.org/10.1016/j.enconman.2015.12.063.

[6] Mikalsen R, Roskilly AP. A review of free-piston engine history and applications. Appl Therm Eng 2007;27(14):2339–52. http://dx.doi.org/10.1016/j.

[7] Huihua Feng, Chendong Guo, Chenheng Yuan, et al. Research on combustion process of a free piston diesel linear generator. Appl Energy 2016;161:395–403. http://dx.doi.org/10.1016/j.apenergy.2015.10.069.

[8] Lim Ocktaeck, Hung Nguyen Ba, Seokyoung Oh, et al. A study of operating parameters on the linear spark ignition engine. Appl Energy 2015;160:746–60. http://dx.doi.org/10.1016/j.apenergy.2015.08.035.

[9] Jinlong Mao, Zhengxing Zuo, Huihua Feng. Parameters coupling designation of diesel free-piston linear alternator. Appl Energy 2011;88:4577–89. http://dx.doi.org/10.1016/j.apenergy.2011.05.051.

[10] Mikalsen R, Roskilly AP. The control of a free-piston engine generator. Part 2: Engine dynamics and piston motion control. Appl Energy 2010;87(4):1281–7. http://dx.doi.org/10.1016/j.apenergy.2009.06.035.

[11] Mikalsen R, Jones E, Roskilly AP. Predictive piston motion control in a free-piston internal combustion engine. Appl Energy 2010;87:1722–8.

[12] Li Qingfeng, Xiao Jin, Huang Zhen. Simulation of a two-stroke free-piston engine for electrical power generation. Energy Fuels 2008;22:3443–9.

[13] Pescara RP. Motor compressor apparatus [P];1928.

[14] Achten PAJ. A review of free piston engine concepts. SAE Paper 941776, Society of Automotive Engineers; 1994. p. 1836–47.

[15] Dulpichet Rerkpreedapong. Field Analysis and Design of a Moving Iron Linear Alternator for Use with Linear Engine. Dissertation, West Virginia University; 1999.

[16] Cawthorne W, Famouri P, Clark N. Integrated design of linear alternator/engine system for HEV auxiliary power unit. IEEE Int Electr Machin Drives Conf; 2001. p. 267–74.

[17] Subhash Nandkumar. Two-Stroke Linear Engine. Dissertation, West Virginia University; 1998.

[18] Clark N, Famouri P, Cawthorne W. Operation of a small bore two-stroke linear engine. In: 1998 Fall Technical Conference of The ASME Internal Combustion Engine Division Clymer, New York; September 1998. p. 27–30.

[19] Atkinson C, Petreanu S, Clark N, et al. Numerical Simulation of a Two-Stroke Linear Engine-Alternator Combination. SAE Technical Paper 1999–01-0921; 1999.

[20] Famouri P, Cawthorne WR, Clark N, et al. Design and testing of a novel linear alternator and engine system for remote electrical power system. Power Engineering Society 1999 Winter Meeting, IEEE, http://dx.doi.org/10.1109/PESW.1999.747434.

[21] Van Blarigan P, Paradiso N, Goldsborough S. Homogeneous Charge Compression Ignition with a Free Piston: A New Approach to Ideal Otto Cycle Performance. SAE Paper 982484; 1998.
[22] Nemecek P, Sindelka M,Vysoky O. Control of two-stroke free-piston generator. In: The 6th Asian Control Conference; 2006.
[23] Kock F, Haag J, Friedrich H. The free piston linear generator – development of an innovative, compact highly efficient range-extender module, SAE Technical Paper 2013–01-1727; 2013.
[24] Haag J, Ferrari C, Starcke J, Stöhr M et al. Numerical and experimental investigation of in-cylinder flow in a loop-scavenged two-stroke free piston engine, SAE Technical Paper 2012–32-0114; 2012.
[25] Ferraril Cornelius, Friedrich Horst E. Development of a free-piston linear generator for use in an extended-range electric vehicle. In: EVS26 international battery, hybrid and fuel cell electric vehicle symposium. California, May 6–9; 2012.
[26] Kosaka H, Akita T, Moriya K, Goto S, et al. Development of Free Piston Engine Linear Generator System Part 1 - Investigation of Fundamental Characteristics, SAE Technical Paper 2014–01-1203; 2014.
[27] Goto S, Moriya K, Kosaka H, Akita T, et al. Development of Free Piston Engine Linear Generator System Part 2 - Investigation of Control System for Generator,SAE Technical Paper 2014–01-1193; 2014.
[28] Mikalsen R, Roskilly AP. A computational study of free-piston diesel engine combustion. Appl Energy 2009;86:1136–43. http://dx.doi.org/10.1016/j.apenergy.2008.08.004.
[29] Mikalsen R, Roskilly AP. The design and simulation of a two-stroke free-piston compression ignition engine for electrical power generation. Appl Therm Eng 2008;28:589–600. http://dx.doi.org/10.1016/j.applthermaleng.2007.04.009.
[30] Mikalsen R, Roskilly AP. The control of a free-piston engine generator. Part 1: Fundamental analyses. Appl Energy 2010;87(4):1273–80. http://dx.doi.org/10.1016/j.apenergy.2009.06.036.
[31] Mikalsen R, Roskilly AP. Performance simulation of a spark ignited free-piston engine generator. Appl Therm Eng 2008;28:1726–33. http://dx.doi.org/10.1016/j.applthermaleng.2007.11.015.
[32] Mikalsen R, Roskilly AP. Coupled dynamic-multidimensional modeling of free-piston engine combustion. Appl Energy 2009;86:89–95. http://dx.doi.org/10.1016/j.apenergy.2008.04.012.
[33] Song Yu. Research on key problems for continuous work of compression ignition free-piston engine based on linear generator. Dissertation, Beijing Institute of Technology; 2017.
[34] Jia Boru, Tian Guohong, Feng Huihua, et al. An experimental investigation into the starting process of free-piston engine generator. Appl Energy 2015;157:798–804. http://dx.doi.org/10.1016/j.apenergy.2015.02.065.
[35] Jia Boru, Zuo Zhengxing, Feng Huihua, Tian Guohong, Roskilly AP. Investigation of the starting process of free-piston engine generator by mechanical resonance. Energy Procedia 2014;61:572–7. http://dx.doi.org/10.1016/j.egypro.2014.11.1173.